Investigation of the magnetocaloric effect and phase transition in a newly discovered perovskite oxide $La_{0.7}Ba_{0.25}Nd_{0.05}Mn_{1-x}Zn_xO_3$ for x = 0.03 and 0.05.

Biswajit Dey[1], *Arnab Basu*[2*], *Soumyadipta Pal*[2], *Sanjay Kumar*[1]

[1]Department of Physics, Jadavpur University, Kolkata-700032, India

[2]Institute of Engineering & Management, University of Engineering and Management, Kolkata-700091, India

Abstract. In this study, we examine the magnetocaloric behavior of the newly discovered perovskite oxide $La_{0.7}Ba_{0.25}Nd_{0.05}Mn_{1-x}Zn_xO_3$ (x = 0.03 and 0.05). We focus on key magnetocaloric parameters, such as magnetic entropy change, heat capacity change, full-width at half-maximum (FWHM), and relative cooling power (RCP) by analysing the temperature-dependent magnetization using a phenomenological model. The impact of Zn doping on both the magnetic properties and the magnetocaloric effect (MCE) is also investigated. As Zn concentration increases, the ferromagnetic to paramagnetic (FM-PM) transition temperature (T_C) decreases, indicating a suppression of the magnetic behaviour. Notable changes in entropy and specific heat are observed around T_C. We predict the MCE parameters by calculating the temperature-dependent magnetization data with varying external magnetic fields (H) using the model. The RCP values are 338.80 J / kg for x = 0.03 and 335.44 J / kg for x = 0.05 at a magnetic field of 50 kOe. All the results suggest that the material holds significant potential for magnetic refrigeration (MR) applications over a broad temperature range near room temperature. The Arrott plots confirm the second-order phase transition (SOPT) between the ferromagnetic and paramagnetic phases. Furthermore, the accuracy of the results and the reliable predictions of the MCE parameters validate the effectiveness of the phenomenological model.

1 Introduction

The study of magnetocaloric effect imparts a clear grasp of fundamental physics, particularly in magnetism and thermodynamics. Recently this study of MCE attracts the researchers for its potential to revolutionize cooling technologies, enhance energy efficiency, promote environmental sustainability and open up new avenues for scientific and technological advancements. This research contributes to a broader understanding of material properties and can lead to breakthroughs in other scientific and engineering fields. MCE is the foundation of magnetic refrigeration (MR) devices. MR is a promising technology over traditional cooling system which relies on gas compression and expansion for its higher efficiency, more precise temperature control and most importantly for the green sustainability. MCE refers to the intrinsic property of all magnetic materials, demarcated as the reversible change in magnetic entropy when a material is subjected to a varying magnetic field [1]. When exposed to an external magnetic field, the magnetic moments of the material align quickly. This alignment restricts the movements of the magnetic moment, resulting in decrease the magnetic entropy. While the lattice and electronic entropies are increasing to maintain the total entropy of the magnetic system constant. Leading to an increase in the material's temperature. After removing the magnetic field, the magnetic moments are relaxed and the material experiences a cooling effect. The advance of MR technology, based on this principle, is still in its early stages. Consequently, scientists are looking for novel compounds with superior MCE qualities [2].

*Corresponding author: A. Basu (basuarnab1990@gmail.com)

From the very beginning several investigations were carried out on the material to obtain high MCE, such as Gd, $Gd_5Si_2Ge_2$, $Gd_5(Si_xGe_{1-x})_4$, MnP, NiMnGa alloys, MnAsSb alloys, LaFeCoS alloys, MnFePAs alloys and others. Recently, perovskite manganites with the general formula $Re_{1-x}A_xMnO_3$ (where Re = La, Pr, Nd, Sm; A = Ca, Sr, Ba, Na, K) have acquired noteworthy attention for its promising potential in various magnetic field applications, together with MR, sensors, thermal management in electronics, cryogenics, magnetic heat pumps and infrared detectors. These materials are widely studied in context of MR because of its huge entropy changes, excellent chemical steadiness, high resistivity and less production costs [3].

In lanthanum manganites, the electric and magnetic properties, particularly around the phase transition and magnetocaloric effect, are strongly influenced by the ferromagnetic double-exchange (DE) interaction and Jahn-Teller (JT) distortions. The intensity of these interactions relies on the Mn^{3+} to Mn^{4+} ratio and the material's structural parameters [4-5]. Studies have demonstrated that partial substitution of La or Mn sites in manganites can modify the magnetic ordering as well as modulate the strength of the DE interactions in the Mn^{3+}–O–Mn^{4+} coupling. Numerous studies have explored the effects of substituting Mn sites with transition metal ions at varying concentrations [6]. In this work, we focus on perovskite manganites where Zn is partially substituted at Mn sites, specifically in $La_{0.7}Ba_{0.25}Nd_{0.05}Mn_{1-x}Zn_xO_3$ (LBNMZnO) for x = 0.03 and 0.05, to investigate the magnetic phase transition and MCE. These compounds display a curie temperature T_C in the vicinity of room temperature and undergo the SOPT. This phase conversion is accompanied by a significant magnetic entropy change, positioning them favourable for applications in MR. Notably, the MCE of this specific perovskite manganite has not been previously explored. We apply a phenomenological model proposed by Hamad [7-8] to simulate the temperature dependency of magnetization and to predict the MCE properties. The essential parameters for evaluating refrigeration, such as magnetic entropy change (ΔS^M), heat capacity change (ΔC_H), FWHF (δT_Γ) and relative cooling power (RCP) are analysed. This study represents the first theoretical analysis of these MCE properties for $La_{0.7}Ba_{0.25}Nd_{0.05}Mn_{1-x}Zn_xO_3$ (x = 0.03 and 0.05). Our predicted values are compared with experimental results and values from other perovskite materials. Overall, our findings are reliable for evaluating MCE at room temperature. Additionally, the results demonstrate the usefulness of the phenomenological model in accurately forecasting the MCE parameters.

2 Theoretical Formulation

We theoretically discuss the magnetocaloric properties and phase transition of LBNMZnO. For this description, we use the phenomenological model which is proposed by Hamad et al. [7-8]. According to the model, the dependence of magnetization (M) on temperature T and Curie temperature T_C is expressed by,

$$M = \frac{M_{initial}-M_{final}}{2}\, tanh\,[\alpha(T_C - T)] + \beta T + \gamma \tag{1}$$

here $M_{initial}$ and M_{final} are the initial and final magnetization value at a constant magnetic field, near the FM-PM phase transition, respectively; $\alpha = \frac{2(\beta - S_C)}{M_{initial}-M_{final}}$; $\beta = \left(\frac{dM}{dT}\right)_{T\approx T_{init}}$ is magnetization sensitivity *(dM / dT)* at temperature $T = T_{init}$ at the ferromagnetic state before transition. In this case $M_{initial}$ is developed already. Besides, $S_C = \left(\frac{dM}{dT}\right)_{T=T_C}$ is magnetization sensitivity at T_C; $\gamma = \frac{M_{initial}+M_{final}}{2} - \beta T_C$.

For a magnetic system, the magnetic entropy change (ΔS^M) under adiabatic magnetic field variation can be calculated by:

$$\Delta S^M = \int_0^{H_{max}} \left(\frac{\partial M}{\partial T}\right)_H dH$$

After performing the integration, we obtain,

$$\Delta S^M = \left\{-\alpha\, \frac{M_{initial}-M_{final}}{2}\, sech^2\,[\alpha(T_C - T)] + \beta\right\} H_{max} \tag{2}$$

From Eq. (2), we explicitly state that ΔS^M increases with increase in magnetization sensitivity at T_C. The high magnetic moment and the swift change in magnetization at T_C are responsible for the significant magnetic entropy change. At T_C, the maximum entropy change (ΔS^M_{max}) is given by:

$$\Delta S_{max}^{M} = H_{max}\left(-\alpha\left(\frac{M_{initial}-M_{final}}{2}\right)+\beta\right) \quad (3)$$

For evaluating the magnetic cooling efficiency and the full-width at half-maximum (δT_Γ), Eq. (3) plays a crucial role. δT_Γ is derived as [9]:

$$\delta T_\Gamma = \frac{2}{\alpha}\, cosh^{-1}\left(\sqrt{\frac{2\alpha(M_{initial}-M_{final})}{\alpha(M_{initial}-M_{final})+2\beta}}\right) \quad (4)$$

Eq. (4) directs that δT_Γ decreases with an increase in α and with a decrease in the difference ($M_{initial} - M_{final}$). This equation provides the full-width at half-maximum magnetic entropy change, which contributes to the evaluation of magnetic cooling efficiency. The product of two quantities ΔS and δT_Γ is known as the relative cooling power (RCP), can be carried out as:

$$RCP = \left(M_{initial} - M_{final} - \frac{2\beta}{\alpha}\right)H_{max} \times cosh^{-1}\left(\sqrt{\frac{2\alpha(M_{initial}-M_{final})}{\alpha(M_{initial}-M_{final})+2\beta}}\right) \quad (5)$$

Moreover, the change in specific heat due to magnetization is presented by:

$$\Delta C_H = T\frac{\delta\Delta S}{\delta T} \quad (6)$$

Since dM / dT < 0, $\Delta S^M < 0$ and therefore, the total entropy decreases with magnetization. Furthermore, $\Delta C_H < 0$ for $T < T_C$ and $\Delta C_H > 0$ for $T > T_C$. The specific heat change can be derived as [9]:

$$\Delta C_H = -T\alpha^2(M_{initial} - M_{final})\, sech^2[\alpha(T_C - T)] \times tanh[\alpha(T_C - T)]H_{max} \quad (7)$$

3 Results and Discussion

The dependenc of magnetization (M) on temperature for LBNMZnO compounds with x = 0.03 and 0.05 is shown in Figure 1, under varying magnetic fields ranging from H = 5 kOe to H = 50 kOe (with a step size of ΔH = 5 kOe). The magnetic phase transition from paramagnetic to ferromagnetic phase takes place as temperature lowers, that is clearly illustrated in Figure 1. The symbols in the figure signify experimental data of the M vs μ_0H plots for (a) LBNMZnO-003 (x = 0.03) and (b) LBNMZnO-005 (x = 0.05) [10]. The continuous lines correspond to the fitted curves obtained using Eq. (1) based on the phenomenological model. The fitting results provide the specific model parameters, which are summarized in Table 1. These parameters are useful while calculating the magnetocaloric properties.

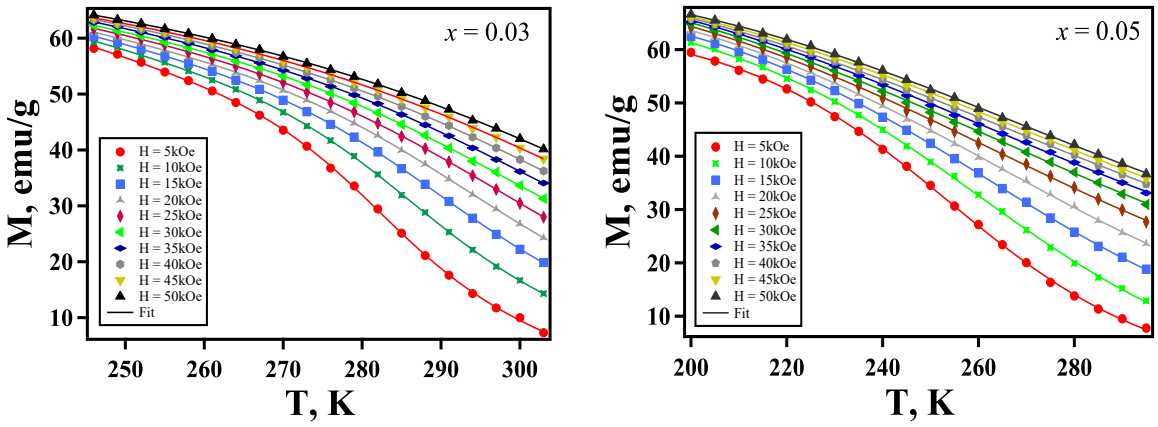

Figure 1. The temperature-dependent magnetization for x = 0.03 and 0.05 with varying magnetic field from H = 5 kOe to 50 kOe. The various symbols characterize the experimental data taken from [10] and the continuous curves correspond to modelled results.

It is clearly observed that for a given magnetic field, the transition temperature (T_C) for x = 0.03 is higher than the values for x = 0.05. The reduction in T_C values for x = 0.05 is linked to a decline in the double-exchange interaction. In contrast, for x = 0.03, an increase in T_C with growing magnetic field is noted, resulting from the enhancement in the exchange coupling among the dipoles as the field intensifies. However, for x = 0.05, fluctuations are seen at specific magnetic fields (20 kOe and 30 kOe). These fluctuations are likely caused by the significant substitution of Zn^{2+} ions, which modifies Mn^{3+}/Mn^{4+} ratio, thereby suppressing the DE interaction [11].

Table 1. The modelled fitting parameters for x = 0.03 and 0.05 with H ranging from 5 kOe to 50 kOe.

Composition x	H (kOe)	$M_{initial}$ (emu/g)	M_{final} (emu/g)	S_C (emu/(g.K))	β (emu/(g.K))	T_C (K)
0.03	5	42.714 ±0.315	14.938± 0.307	-1.3744 ± 0.0083	-0.43728 ± 0.0252	282.26 ± 0.212
	10	44.737 ± 0.465	16.819 ± 0.391	-1.145 ± 0.00927	-0.37573 ± 0.0213	286.18 ± 0.234
	15	46.769 ± 0.546	17.28 ± 0.511	-0.9957 ± 0.00479	-0.32224 ± 0.0165	289.75 ± 0.251
	20	48.817 ± 0.596	16.916 ± 0.642	-0.90003 ± 0.00362	-0.27614 ± 0.0181	293.13 ± 0.295
	25	51.454 ± 0.604	12.507 ± 0.656	-0.83073 ± 0.00541	-0.22377 ± 0.0213	298.12 ± 0.331
	30	50.051 ± 0.729	19.504 ± 0.863	-0.76192 ± 0.00632	-0.25007 ± 0.023	298.47 ± 0.392
	35	50.321 ± 0.826	21.302 ± 0.942	-0.71508 ± 0.00712	-0.24595 ± 0.0254	300.5 ± 0.415
	40	51.152 ± 0.986	16.559 ± 1.34	-0.70514 ± 0.00926	-0.22071 ± 0.0263	306.36 ± 0.461
	45	56.179 ± 1.25	7.377 ± 1.74	-0.67867 ± 0.0103	-0.1492 ± 0.0307	312.87 ± 0.623
	50	55.034 ± 1.86	11.016 ± 1.92	-0.64883 ± 0.0162	-0.1639 ± 0.0353	314.15 ± 0.748
0.05	5	60.663 ± 0.493	2.2016 ± 0.212	-0.74362 ± 0.0071	-0.04874 ± 0.00878	253 ± 0.207
	10	60.75 ± 0.544	4.64 ± 0.304	-0.64596 ± 0.005	-0.088019 ± 0.0095	259.87 ± 0.271
	15	67.464 ± 0.695	4.1272 ± 0.262	-0.55937 ± 0.00244	-0.03986 ± 0.00811	261.73 ± 0.344
	20	71.787 ± 0.72	4.3208 ± 0.296	-0.49042 ± 0.00348	-0.026436 ± 0.0107	264.04 ± 0.379
	25	80.02 ± 1.03	1.9284 ± 0.298	-0.43486 ± 0.0037	-0.020731 ± 0.0173	263.48 ± 0.447
	30	79.192 ± 1.312	6.0584 ± 0.441	-0.39469 ± 0.00357	-0.01025 ± 0.0271	265.17 ± 0.598
	35	80.906 ± 1.69	8.6313 ± 0.523	-0.37614 ± 0.00379	-0.010084 ± 0.0259	263.59 ± 0.756
	40	85.372 ± 2.27	3.2236 ± 0.59	-0.36292 ± 0.00294	0.028243 ± 0.0262	268.46 ± 0.954
	45	89.198 ± 2.21	1.2787 ± 0.413	-0.3613 ± 0.00248	0.073412 ± 0.0274	268.63 ± 1.2
	50	89.236 ± 2.45	2.8 ± 0.346	-0.3586 ± 0.00245	0.082013 ± 0.0258	268.74 ± 1.96

Figure 2. illustrates the temperature dependency of the modelled magnetic entropy change (ΔS^M) for LBNMZnO at different fields, using the parameters fitted in Eq. (2). It is clear that a substantial change in entropy develops at transition temperature (T_C), influenced by the strong magnetic moment and swift variations in magnetization. This leads to a notable variation in entropy with changing magnetic field. As the magnetic field increases, the peak position shifts toward higher temperatures for x = 0.03. However, for x = 0.05, deviations from this trend are observed. These deviations may arise from the compression of the PM-FM transition. This compression occurs due to the alignment of magnetic spins along the applied magnetic field. Furthermore, the peak of the entropy change (ΔS^M_{max}) near Curie temperature becomes more pronounced as the magnetic field strength increases for both compositions. The values of ΔS^M_{max} are calculated using Eq. (3) and summarized in Table 3. Notably, partial Zn^{2+} substitution in Mn site meaningfully reduces ΔS^M. The extreme value of magnetic entropy change (ΔS^M_{max}) for x = 0.03 is approximately -3.3242 J / (kg·K), while for x = 0.05, its around -1.8230 J / (kg·K). The suppression of ΔS^M_{max} due to the partial substitution of Zn^{2+} (non-magnetic). Due to this substitution the Mn^{3+}-O-Mn^{4+} pairs reduce that enhances antiferromagnetic coupling and distorts the bond length and angle of Mn–O–Mn. Thus, the spin-lattice coupling is crucial in driving the significant entropy change observed in perovskites during the magnetic ordering process [12]. Furthermore, we compare the experimental ΔS^M_{max} values with those predicted by the model at 50 kOe, and find them to be in good agreement (Table 2). The ΔS^M_{max} values in this study are comparable to those found in other perovskite oxides with large magnetocaloric effects [13-14]. The patterns of entropy change provide insights into controlling the temperature range for refrigeration applications. Overall, these outcomes specify the material holds great promise in MR technologies in the near room temperature range.

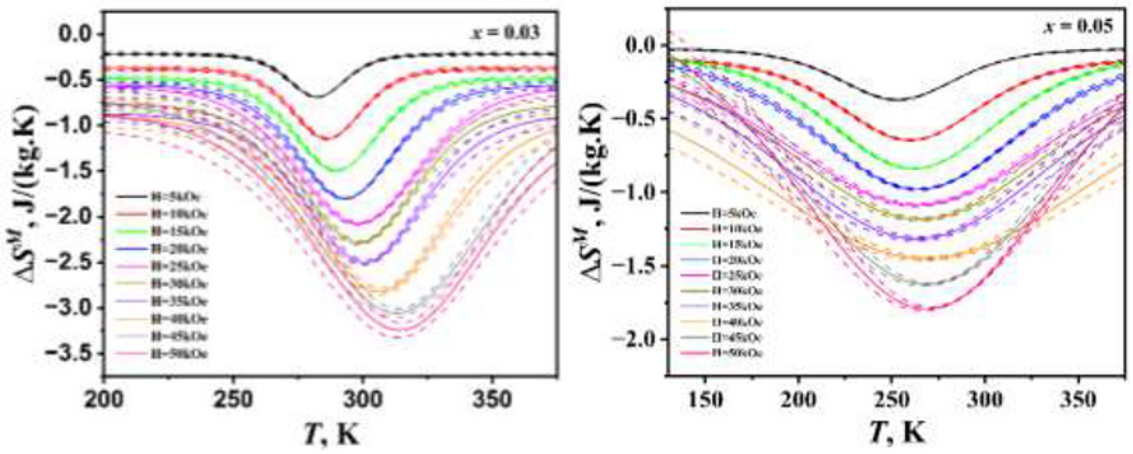

Figure 2. The variation of magnetic entropy changes with temperature for $x = 0.03$ and 0.05 as H varies from 5 kOe to 50 kOe. The broken lines show the predicted range of variation of ΔS^M.

Table 2. Comparison between experimental and theoretical values of maximum entropy change at 50 kOe magnetic field.

Compound	Experimental Value	Theoretical Values (Our Work)
$La_{0.7}Ba_{0.25}Nd_{0.05}Mn_{0.97}Zn_{0.03}O_3$	-3.96 J/(kg.K)	-3.3242 J/(kg.K)
$La_{0.7}Ba_{0.25}Nd_{0.05}Mn_{0.95}Zn_{0.05}O_3$	-2.27 J/(kg.K)	-1.8230 J/(kg.K)

We are looking for materials capable of transporting heat across a significant temperature difference between the reservoirs in an ideal refrigeration cycle. To this end, we investigate another key magnetocaloric effect (MCE) property, namely the change in heat capacity (ΔC_H). Figure 3. presents the temperature dependency of the heat capacity change (ΔC_H) for LBNMZnO at different magnetic fields, using the parameters fitted in Eq. (7). We can observe a sharp change in ΔC_H from minimum value to maximum value at T_C. A material with a sharp and large change in its specific heat near the transition temperature will typically show a higher ΔS^M and, consequently, a more pronounced MCE. This is because the large specific heat means that more heat is either absorbed or released as the magnetic field changes. In this case the change in specific heat is considerable in high magnetic field, which indicates this material as one of the auspicious candidates for cooling appliances. However, the change in specific heat is higher for $x = 0.03$ than for $x = 0.05$. This may occur due to the suppression of the PM-FM transition, caused by the arrangement of magnetic spins with magnetic field, resulting from the relatively high doping of Zn in Mn site.

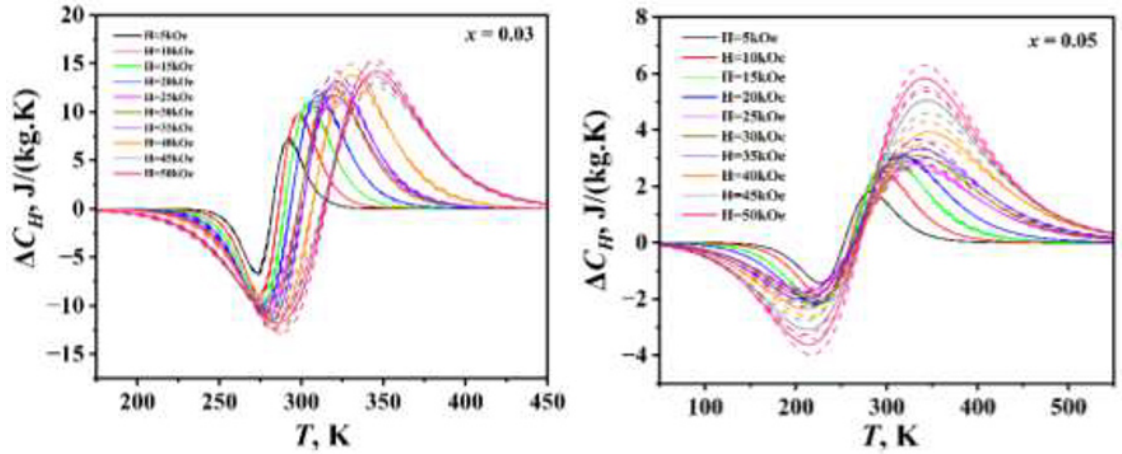

Figure 3. The variation of heat capacity changes with temperature for x = 0.03 and 0.05 as the magnetic field varies from H = 5 kOe to 50 kOe. The broken lines show the predicted range of variation of ΔC_H.

Table 3. The predicted values of maximum magnetic entropy change (ΔS^M_{max}), FWHM (δT_Γ), relative cooling power (RCP) and maximum heat capacity change (ΔC_{Hmax}) for x = 0.03 and 0.05 as the magnetic field varies from H = 5 kOe to 50 kOe (with errors).

Composition x	**H (kOe)**	ΔS^M_{max} **(J / (kg.K))**	δT_Γ **(K)**	**RCP (J / kg)**	ΔC_{Hmax} **(J / (kg.K))**
0.03	5	-0.6872 ± 0.0042	37.9223 ± 1.823	26.0602 ± 1.4105	-6.6291 ± 0.2493 7.1069 ± 0.2541
	10	-1.1450 ± 0.0093	47.3139 ± 2.072	54.1745 ± 2.8119	-8.9414 ± 0.2691 9.7242 ± 0.2771
	15	-1.4935 ± 0.0072	56.5972 ± 2.5251	84.5306 ± 4.1788	-9.7847 ± 0.3461 10.8029 ± 0.3631
	20	-1.8001 ± 0.0073	64.1009 ± 3.7136	115.3854 ± 7.1502	-10.3909 ± 0.5201 11.6474 ± 0.5220
	25	-2.0769 ± 0.0135	75.6757 ± 4.8482	157.1652 ± 11.0962	-10.101 ± 0.5739 11.6379 ± 0.6159
	30	-2.2858 ± 0.0190	77.8147 ± 7.0485	177.8656 ± 17.5978	-11.0562 ± 0.8131 12.6123 ± 0.8606
	35	-2.5028 ± 0.0250	83.2329 ± 9.2487	208.3134 ± 25.146	-11.4655 ± 0.9912 13.125 ± 1.0558
	40	-2.8206 ± 0.0370	90.5106 ± 9.6051	255.2907 ± 29.4766	-11.8395 ± 1.0166 13.8014 ± 1.0861
	45	-3.0541 ± 0.0464	101.4041 ± 10.5179	309.6896 ± 36.862	-11.279 ± 1.0630 13.6906 ± 1.1559
	50	-3.3242 ± 0.0810	104.4332 ± 11.5925	338.7969 ± 46.157	-11.7263 ± 1.0172 14.1778 ± 1.1149
0.05	5	-0.3719 ± 0.0036	78.4036 ± 0.6047	29.1513 ± 0.5032	-1.4384 ± 0.0009 1.7896 ± 0.0017
	10	-0.6460 ± 0.0050	100.3860 ± 1.8168	64.8454 ± 1.6982	-1.9481 ± 0.0263 2.5119 ± 0.0308
	15	-0.8391 ± 0.0037	114.2071 ± 1.9465	95.8260 ± 2.0514	-2.1998 ± 0.0425 2.9863 ±0.0531
	20	-0.9809 ± 0.0070	134.1046 ± 3.7865	131.5352 ± 4.6479	-2.1515 ± 0.0609 3.0862 ± 0.0756
	25	-1.0872 ± 0.0092	172.9625 ± 10.0365	188.0362 ± 12.516	-1.7438 ± 0.1121 2.7821 ± 0.1467
	30	-1.1841 ± 0.0107	171.2785± 18.4589	202.8057 ± 23.7104	-1.9368 ± 0.2433 3.0933 ± 0.3155
	35	-1.3286 ± 0.0133	178.8932 ± 18.3014	236.6510 ± 26.4768	-2.038 ± 0.2442 3.3213 ± 0.3232
	40	-1.4517 ± 0.0118	177.3536 ± 15.9515	257.3959 ± 25.2227	-2.3555 ± 0.2677 3.9213 ± 0.3625
	45	-1.6259 ± 0.0113	184.9366 ± 12.9604	300.9036 ± 22.8126	-3.0916 ± 0.3356 5.051 ± 0.453
	50	-1.8230 ± 0.0123	184.0407 ± 10.6113	335.4370 ± 20.8491	-3.6201 ± 0.3551 5.8283 ± 0.474

Furthermore, the values of FWHM (δT_Γ), relative cooling power (RCP), maximum heat capacity change (ΔC_{Hmax}) along with maximum magnetic entropy change (ΔS^M_{max}) are calculated using the Eq. (4), Eq. (5), Eq. (7) and recorded in Table 3. These are crucial parameters for arbitrating the effectiveness of a refrigerant material. The forecasted peak value of ΔS^M for changes from ~ -0.6872 J / (kg.K) to ~ -3.3242 J / (kg.K) for x = 0.03 and for x = 0.05, it changes from ~ -0.3719 J / (kg.K) to ~ -1.8230 J / (kg.K) with the magnetic field ranging from 5 kOe to 50 kOe. Now, the RCP takes the values in the range of ~ 26.0602 J / kg to ~ 338.7969 J / kg for x = 0.03 and for x = 0.05, it changes from ~ 29.1513 J / kg to ~ 335.4370 J / kg with changing magnetic field from 5 kOe to 50 kOe. The performance of the system in refrigeration is enumerated by RCP values and we witness the RCP values are considerably high for these materials. Again, as magnetic field increases the RCP values are increasing for both compound which is depicted in Figure 4.

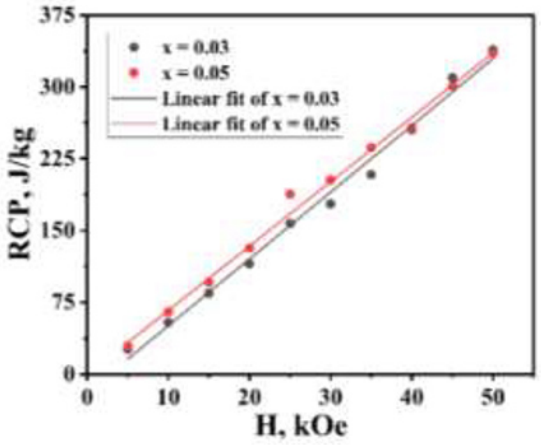

Figure 4. Field dependency of RCP with varying magnetic field from 5 kOe to 50 kOe

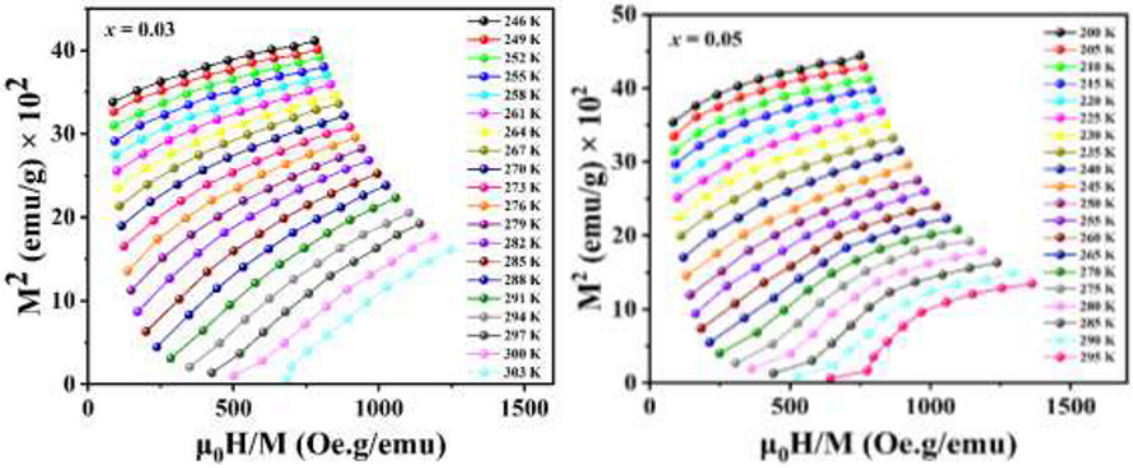

Figure 5. Arrott plots for x = 0.03 and 0.05.

It is obvious that, with increasing magnetic field, the values of the MCE parameters generally increase, except in certain cases for x = 0.05. This can be attributed that a higher magnetic field induces greater magnetization and enhances the change during the FM-PM phase transition, which is primarily a SOPT. The nature of the magnetic transition can be described using Arrott plots (M^2 vs $\mu_0 H/M$ plot) following Banerjee's criterion [15]. The Arrott plots of LBNMZnO compound are depicted in Figure 5. As we can see from the plots, all the curves exhibit positive slope over wide temperature range, demonstrating a SOPT for x = 0.03. However, for x = 0.05, some curves are not linear at higher temperatures above T_C, indicating non-homogenic character of SOPT. Overall, the calculated MCE parameters indicate that the LBNMZnO compound holds significant potential as MCE compound for solid-state refrigeration applications.

4 Conclusion

The magnetocaloric effect of LBNMZnO compounds are investigated in vicinity T_C. Using the extracted data from reference [10], we plot the temperature-dependent magnetization curves with magnetic fields varying from 5 kOe to 50 kOe, which is based on the phenomenological model. Using the phenomenological model-based equations, we forecast the magnetocaloric characteristics. These compound poses curie temperature near room temperature and exhibit SOPT with effective magnetic entropy changes. We get the FM-PM transition temperature is decreasing with an increase in partial substitution of Zn in Mn sites due to the reduction of DE interaction. The transition temperature is ranging from 260 K to 315 K approximately. These compounds exhibit a significant magnetocaloric effect (MCE) within this temperature range, enhancing their relevance. The variations in magnetic entropy and specific heat near T_C suggest a notable shift in magnetization, potentially indicating a transition in the

material's magnetic phase from first order to second order. The ΔS^{M}_{max} values for x = 0.03 is ~ -3.3242 J / (kg.K) and for x = 0.05 is ~ -1.8230 J / (kg.K) at 50 kOe. The maximum values are notable and comparable to those observed in other similar types of perovskites. The large values of RCP show the better cooling efficiency. According to the Arrott plots, both the compound experiences a SOPT. Moreover, in this work all the calculations are carried out using the phenomenological model, which is proposed by Hamad with less computational efforts and the results we get are promising and comparable with the experimental paper [10]. These results are also comparable with other perovskite oxides. Thus, we can effectively explore the magnetocaloric effects of the materials based on the phenomenological model. We can conclude that we investigate the magnetocaloric effect of LBNMZnO and highlight these compounds as promising prospects among perovskite oxides for applications in refrigeration and various other technologies across a broad temperature range near room temperature. Additionally, we highlight the effectiveness of the phenomenological model in describing their behaviour.

REFERENCES

1. V.K. Pecharsky, K.A. Gschneidner Jr., J. Appl. Phys. **86**, 565 (1999).
2. Y. Tomioka, T. Ito, A. Sawa, J. Phys. Soc. Jpn. **84**, 024703 (2015).
3. M.H. Phan, S.C. Yu, Review of the magnetocaloric effect in manganite materials, J. Magn. Magn Mater. **308** (2), 325–340 (2007), https://doi.org/10.1016/j.jmmm.2006.07.025.
4. John-Teller, M. B. Salamon, and M. Jaime, Reviews of Modern Physics **73** (3), 583–628 (2001).
5. M. H. Phan, V. Franco, N. S. Bingham, H. Srikanth, N. H. Hur, and S. C. Yu, Journal of Alloys and Compounds **508**, 238–244 (2010).
6. A. Cos ¸kun, E. Tas ¸arkuyu, A.E. Irmak, M. Acet, Y. Samancio ̆lu, S. Aktürk, Magnetic properties of La0.65Ca0.30Pb0.05Mn0.9B0.1O3 (B = Co, Ni, Cu and Zn), J. Alloys Compd. **622**, 796–804 (2015), https://doi.org/10.1016/j.jallcom.2014.10.182.
7. M.A. Hamad. Phase Trans. Journal of Advanced Ceramics 2012, **1**(4): 290-295. DOI: 10.1007/s40145-012-0027-8.
8. A.H. El-Sayed, M.A. Hamad. J. Supercond. Nov. Magn. **31**, 10, 3357 (2018). https://doi.org/10.1007/s10948-019-05232-3.
9. S. Pal, S. Datta. J. Supercond. Nov. Magn. **34**, 11, 2905 (2021). https://doi.org/10.1007/s10948-021-06020-8.
10. D.R. Munazat, B. Kurniawan, D.S. Razaq, M. Manawan, W.H. Shon, J.S. Rhyee, D. Nanto. Effect of Zn substitution on magnetic properties and magnetic entropy change in La0.7Ba0.25Nd0.05Mn1-xZnxO3 (x=0.03 and 0.05) synthesized by using sol-gel method. Physica B: Condensed Matter, **679**, 415800 (2024), https://doi.org/10.1016/j.physb.2024.415800.
11. F. Gong, W. Tong, S. Tan, Y. Zhang, Large effect of small Zn doping on the electric and magnetic properties in LaMn1-xZnxO3, Phys. Rev. B Condens. Matter **68**, (17), 2–7 (2003), https://doi.org/10.1103/PhysRevB.68.174410.
12. Z.B. Guo, Y.W. Du, J.S. Zhu, H. Huang, W.P. Ding, D. Feng, Large magnetic entropy change in perovskite-type manganese oxides, Phys. Rev. Lett. **78** (6), 1142–1145 (1997), https://doi.org/10.1103/PhysRevLett.78.1142.
13. C.G. Ünlü, *et al.*, Magnetocaloric effect in La0.7NdxBa(0.3-x)MnO3(x = 0, 0.05, 0.1) perovskite manganites, J. Alloys Compd. **704**, 58–63 (2017), https://doi.org/10.1016/j.jallcom.2017.02.030.
14. Z. Xie, et al., Structural, magnetic, and magnetocaloric properties of La0.7Sr0.2Nd0.1Mn1-xNixO3 (x= 0.05, 0.10, and 0.15): B-site doping, Phys. B Condens. Matter **639,** (2022), https://doi.org/10.1016/j.physb.2022.413985.
15. B.K. Banerjee, On a generalised approach to first and second order magnetic transitions, Phys. Lett. **12** (1), 16–17 (1964), https://doi.org/10.1016/0031-9163(64)91158-8.